Pseudomonas aeruginosa initiates a rapid and specific transcriptional response to surfaces during biofilm initiation

Undergraduate Research Thesis

Presented in partial fulfillment of the requirements for graduation with honors research distinction in the undergraduate colleges of The Ohio State University

By

Nikolas Grotewold

The Ohio State University

April 2020

Honors Thesis Committee:

Project Advisor: Dr. Daniel Wozniak, Department of Microbial Infection & Immunity

Dr. Venkat Gopalan

Dr. Paul Stoodley

Abstract

Pseudomonas aeruginosa forms complex cell aggregates, called biofilms, through production of exo-polysaccharides that form a thick, protective mucoid layer. Biofilms have serious health implications for immunocompromised patients, resulting in increased mortality rates for burn wound, Cystic Fibrosis (CF), AIDS, and chemotherapy patients. While many studies have focused on mature biofilms, this thesis explores the initial cell-surface interactions that allow for the establishment of the biofilm. The early steps of surface attachment remain obscure, with little information present on how planktonic cells transition to biofilm cells, and the signaling cascade and regulation networks that mediate this phenotypic change. The aim of this study was to define the kinetics of *P. aeruginosa* transcriptional response to a surface and identify key genes that play a role in the attachment process. An mRNA analysis of *P. aeruginosa* at various time points post-attachment revealed genes involved in this process. A mutant library of these genes was used to perform lengthened biofilm crystal violet assays, indicating which mutants displayed biofilm defects. Four genes (*leuD, phnA, pfpI,* and *moaE*) were analyzed further through complementation assays and growth curve analyses. We propose that these studies present an important background for understanding the initial stages of cell attachment and biofilm formation that may be exploited in future developments of bacterial control strategies and therapies.

Acknowledgements

The results of this *Pseudomonas aeruginosa* surface attachment study have been incorporated into a manuscript that will be submitted to the Journal of Bacteriology.

I would like to thank Dr. Daniel Wozniak for accepting me into his lab when I was a freshman and supporting my research interest throughout the last four years. Dr. Wozniak met with me frequently and set aside much time to help me develop the ideas to my project and plan the appropriate experiments. Dr. Wozniak afforded me the opportunity to travel to the local conference hosted by the Ohio Branch of the American Society for Microbiology (ASM) as well as to present at the 8th ASM International Conference on Biofilms in Washington D.C. Throughout the time at lab, I have learned an innumerable number of microbiology techniques and concepts that will serve as the base to my future research. I have greatly enjoyed being in the laboratory during these past four years and I credit my eagerness and growth to the support and enthusiasm that Dr. Wozniak has extended to my learning. Dr. Wozniak embodies the definition of a great mentor through his dedication and guidance, and I was very fortunate to have the opportunity to develop as a scientist on his team.

I would also like to thank Dr. Christopher Jones for taking me under his wing at the genesis of my time in lab and for his infinite patience and mentorship. Dr. Jones extended the invitation to collaborate on his project alongside him and constantly supported my continuance of the project even through his relocation to industry. Under the careful review of Dr. Jones, I received the Undergraduate Research Scholarship two consecutive years. Dr. Jones taught me a plethora of microbiology techniques and the path to submitting a research manuscript.

I would also like to thank Dr. Erin Gloag for her continual assistance throughout all four years of my time in lab. Dr. Gloag has served as a source of motivation and has elucidated to me

the many ways of approaching dilemmas, in and out of the lab. Dr. Gloag always pushed me to go one step further than my comfort zone, allowing me to feel truly proud of my scientific accomplishments. I am certain that Dr. Gloag will continue to leave a lasting impact on many more mentees and scholars to come.

I would also like to thank the rest of Dr. Wozniak's lab including Sheri "Mona" Dellos-Nolan, Dr. Landon Locke, Dr. Katarzyna Danis-Wldorczyk, Preston Hill, Yiwei Liu, Pranav Rana, Danielle Ferguson, and Sankalp Malhotra. I greatly appreciate Dr. Paul Stoodley and Dr. Venkat Gopalan for reviewing my thesis and sitting on my thesis defense committee. I would also like to acknowledge my advisor, Dr. Joanna Spanos, and the Honors Advising Committee for their support of my education and research over the last four years.

Lastly, I want to acknowledge my parents, Dr. Andrea Doseff and Dr. Erich Grotewold, for their continued support throughout my education and in supporting my interest in scientific discovery.

Vita

2013-2016	Research Internship, Dr. Jelena Brkljacic, Arabidopsis Biological Resource Center, The Ohio State University
2016 – Present	College of Arts & Sciences Honors Program, The Ohio State University
2016-Present	Maximum Scholarship, The Ohio State University
2016	Caruso Research Scholarship
2017, 2018	Undergraduate Research Scholarship, The Ohio State University
2016-Present	Student Researcher, Dr. Daniel Wozniak Laboratory, The Ohio State University
2018, 2019	Denman Undergraduate Research Forum Presenter, The Ohio State University
2018	Ohio Branch of the American Society for Microbiology Poster Presentation, Ohio University
2018	8th ASM International Conference on Biofilms, Washington D.C.
2017	REU Program with Konstantinos Konstantopoulos, Chemical Bioengineering, in the Institute for NanoBioTechnology, Johns Hopkins University
2017	Oral Presentation for Institute for NanoBioTechnology, Johns Hopkins University
2017	Poster Presentation at C.A.R.E.S. Symposium, Johns Hopkins University
2018	Research Internship with Dr. Grace Chen, Cancer & Immunology, University of Michigan
2019	UM-SMART Research Program with Dr. Sami Barmada, Neurology, University of Michigan

2019	Oral Presentation and Poster Presentation at an Undergraduate Research Symposium, University of Michigan
2020	Bachelor of Science in Biochemistry with Honors Research Distinction, The Ohio State University

Fields of Study

Major Fields: Biochemistry, Pre-Medicine

Minor Fields: Microbiology, Spanish

Table of Contents

1. Introduction

1.1 Nosocomial Infection and Biofilms

Nosocomial infections affect one out of every ten patients admitted to hospitals. These hospital-acquired infections cause increased morbidity and mortality, compounding unaffordable healthcare costs[1]. These infections cause more than a two-fold increase in the length of hospital stays and increased costs of admission, as well as a six-fold increased mortality risk[2]. Complications occurring from catheter- and ventilator-derived infections are primarily biofilm associated[3]. Biofilms have been defined as colonies of bacterial cells that are sessile and irreversibly attached to a substrate, interface, or to each other. Various species differentiate into cell types that interact and cooperate symbiotically for increased survival[4]. Additionally, the cells are covered in a self-produced matrix of extracellular polymer and exhibit modified phenotypes related to growth rate and gene transcription[5]. These communities of adhered microorganisms are recalcitrant to therapy and immune clearance. Biofilms decrease the efficacy of antibiotics, increasing antibiotic resistance by more than 1000-fold and allowing various species to aggregate into a life-threatening infection[6]. Understanding the formation and development of bacterial aggregation is vital to destroying biofilms and preventing fatal hospital-acquired infections. A common organism whose biofilms are associated with a variety of nosocomial infections is *Pseudomonas aeruginosa*.

P. aeruginosa is a model organism in biofilm research due to its success in forming biofilms, its mechanisms for antibiotic resistance, and its medical impact in chronic infections. *P. aeruginosa* is genetically tractable as well and grows quickly and under simple conditions. It is one of the most dangerous hospital-acquired pathogens, thriving in moist environments and augmenting the risk of infection in burn wound, Cystic Fibrosis (CF), AIDS, chemotherapy, and

other immuno-debilitated patients[7]. *P. aeruginosa* is responsible for over 33,000 infection cases and 3,000 deaths each year (CDC). The prevalence of biofilm infections is habitual in these situations, with biofilms detected in up to 95% of ventilator-associated pneumonia (VAP)[8] cases and 80% of adult CF patients[9]. The uncanny ability of *P. aeruginosa* to form virulent biofilms is the main cause for difficulties in treatment and patient complications as production of virulence factors are cell-density dependent and difficult to eradicate[10].

Bacterial biofilms are formed through four main steps (Figure 1): the reversible attachment of bacteria to a surface, the irreversible binding of bacteria where a slime matrix is constructed, the maturation and development of the biofilm structure, and the dispersal of bacterial cells from the biofilm to colonize a new surface. The dispersal of cells can occur through the release of planktonic cells or the separation of part of the biofilm[11]. The formation and survival of a biofilm depends on a strong initial cell-surface attachment to establish initial aggregation. After surface contact, cell adhesion is mediated by way of exo-polysaccharides[12] (including Pel and Psl), adhesins, type IV pili, flagella, regulation by second messengers (cyclic-di-GMP) in signal transduction pathways, and small regulatory RNA (sRNA)[13]. The production of exo-polysaccharides then leads to a thick mucus layer which establishes the foundation for mature biofilm formation. However, the mechanism used by *P. aeruginosa* to sense a surface and the gene expression changes that are associated with surface binding are unclear. Whereas most studies have focused on disrupting biofilms that have already matured, this study is centered around the initiation of bacterial biofilm formation, by identifying genes that are primarily involved in the surface-attachment process.

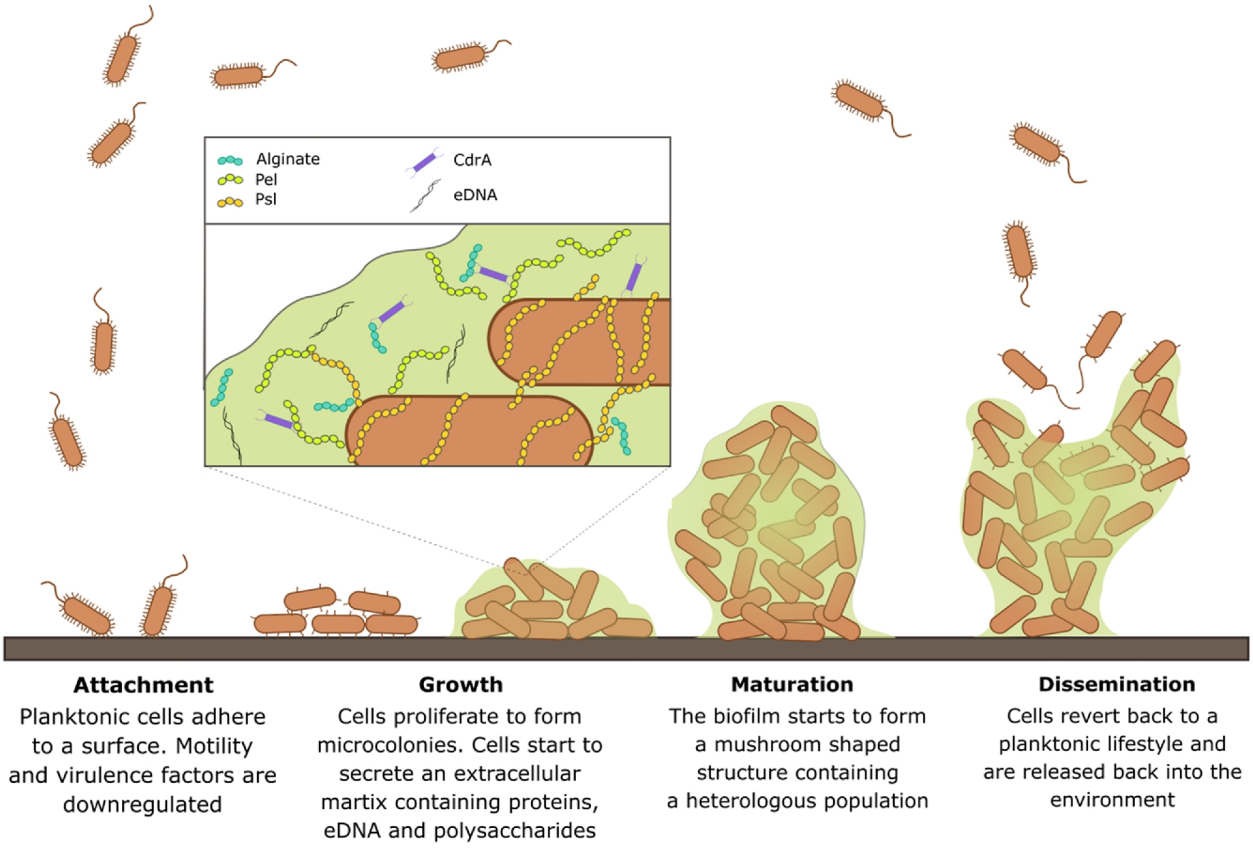

Figure 1 There are four main steps of biofilm formation, described above[11]. This study focuses on the first and second steps of biofilm attachment.

Transcriptional differences between planktonic (motile bacteria) and biofilm populations have previously relied on mature biofilms, and focused studies on samples from 4-12+ h. post-initiation[14,15,16,17,18,19]. While these prior studies have elucidated population changes that occur throughout the biofilm maturation process, this thesis project investigates the initial interactions of bacteria with surfaces. In this study, an optimized RNA-Seq procedure was utilized to generate transcriptional profiles from adherent populations early after surface attachment (5-60 minutes [min]). This approach demonstrated that the transcriptional response began at 15 min after attachment, and peaks at 30 min post-attachment. Subsequently, the genes from the 30-min peak that exhibited the greatest fold-change were studied to identify potential gene functions and prior implications in biofilms. Further exploration of gene relationships with levels of biofilm

production were performed using a transposon library and a high throughput biofilm rapid attachment assay.

1.2 Research motivation and Thesis scope

Mature bacterial biofilms have been studied for decades describing interactions with proteins, polysaccharides, and signaling present in mature structures. Research has identified factors contributing in resistance to antimicrobial agents, sigma factors that activate expression of entire gene collections, and complex microbial communities where each sessile cell is seen to be fundamentally different from planktonic cells of the same species[20]. However, the early events of surface attachment remain obscure. We still lack a full understanding of how planktonic cells transition to biofilm cells, and the signaling cascade and regulation networks that mediate this transition.

The aim of this study was to define the kinetics of *P. aeruginosa* transcriptional response to a surface and identify key genes that play a role in the attachment process. The results will offer an opportunity to identify novel pathways required for bacterial attachment. The first section of this thesis focused on understanding the transcriptional changes that are initiated upon surface attachment of *P. aeruginosa* planktonic cells. Results detailed in this section were performed and analyzed by Dr. Christopher Jones[21]. The second section of this thesis focuses on validating this analysis by determining the role of identified genes in biofilm formation. Results in this section were performed and analyzed by Nikolas Grotewold. The data presented in this thesis will establish the framework for studies of early bacterial responses to surfaces, as well as provide insights to guide targeted molecular studies of *P. aeruginosa* attachment. Results from

this thesis will allow for the development of more effective therapies with greater precision towards preventing fatal biofilm infections.

1.3 Hypothesis

We hypothesized that *P. aeruginosa* detects and senses specific surfaces and initiates a transcriptional response cascade early after attachment, and that modulation of this transcriptional response controls the ability of the bacteria to bind and initiate biofilms.

2. Materials and Methods

2.1 Bacterial Strains and Media

Transposon Library

A commercially available transposon library[22] in the *P. aeruginosa* strain PAO1 background was sourced to pursue phenotypes of genes identified from the RNA-seq analysis. Attachment assays were performed with the transposon mutants of the specific genes that were seen to be most differentially regulated in the RNAseq. PAO1-4317 is the parental strain for the transposon mutants and will be considered the wild type for each of the subsequent experiments in this study. Screening transposon mutants of the most differentially expressed genes prioritized genes critical for the attachment process that merited further study. The transposon mutant strains that were further studied are shown in supplemental table 1.

Media

Luria broth (LB) was prepared by adding 25 grams of pre-mixed Luria broth (Miller) into 1 L of dH_2O. The LB plates were prepared by additionally adding 15 grams of agar per liter.

Vogel-Bonner minimal media (VBMM) contained 0.2g/L $MgSO_4 \cdot 7H_2O$, 3.5g/L $NaNH_4HPO_4 \cdot 4H_2O$, 10g/L K_2HPO_4, 0.1g/L $CaCl_2$, 2g/L citric acid, 1g/L casamino acid.

2.2 RNAseq Analysis of Initial Attachment

RNAseq assays were performed to establish the genes that were most regulated during early bacterial attachment. *P. aeruginosa* planktonic cells were inoculated onto an Ibidi µ-Slide, made up of a thin micro-channel between two plastic slides, and attachment was allowed to occur for 5-60 min, removing cells for transcriptional analysis after the allotted attachment time (Figure 2). Five-minute attachment was considered the baseline where transcriptional changes had not yet occurred; therefore, each time point was compared to the 5-min attachment time point. The period with maximum transcriptional response was noted and mRNAs that were most differentially expressed were explored through further analyses. Bacterial strains with individual disruption in the 30 genes that displayed the highest positive and the 8 genes with the highest negative fold change were further examined by surface attachment assays.

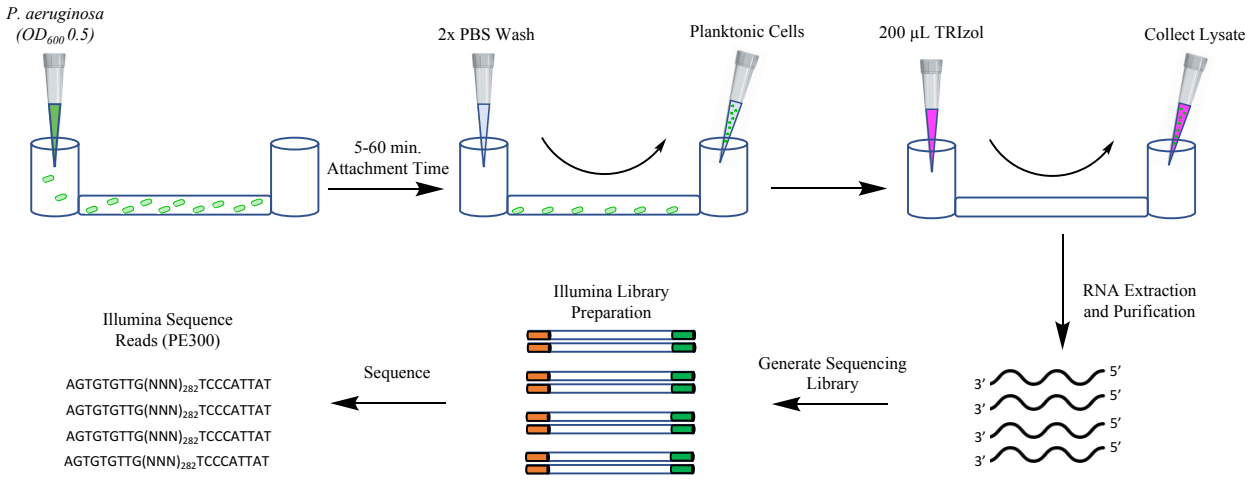

Figure 2 Bacterial attachment was achieved by allowing the cells to adhere for periods of 5-60 min in the micro-channels. Planktonic cells were removed through washes, ensuring that only the attached cells were available for RNA extraction and purification. Multiple attachment experiments were performed for each time point to collect enough RNA for sequencing.

2.3 Biofilm Assays

To quantify biofilm biomass levels, a microtiter crystal violet assay was performed. *P. aeruginosa* strains were grown to mid-log phase (OD_{600}= 0.5) and 100 µL was transferred to a flat-bottom, untreated 96-well microtiter plates (Corning). Biofilms were grown for either three or six hours at 37˚C in a humidified chamber. Biofilms were washed with water to remove unattached cells. The biofilm was then stained with 120 µL of 0.1% (1 g/L) crystal violet and incubated at 25˚C for 30 min. The biofilm was washed in water to remove excess stain. Biofilm-bound crystal violet was extracted in 150 µL of 95% (96.8% v/v) ethanol for 30 min at 25˚C. One hundred µL was transferred to a new microtiter plate and the optical density at 590 nm was measured on a SpectraMax i3 plate reader (Molecular Devices). These values were compared to the isogenic parent PAO1 strain. Significance was determined using a one-way ANOVA, followed by a Dunnett post-hoc test. Four biological replicates, with four technical replicates each were performed.

2.4 Growth Curves

P. aeruginosa strains were grown to OD_{600}= 0.05 and 200 µL of culture were transferred into a sterile 96-well microtiter plate (Corning). Growth was assessed by examining OD_{600} over 20 hour (h) in LB and Vogel-Bonner minimal medium (VBMM), containing 1% (10 g/L) glucose, agar, 1 mM $CaCl_2$, and 1% (10 g/L) carbonic anhydrase. The samples were read every 30 min, with 5 seconds (s) of shaking occurring before each read. Growth occurred at 37˚C throughout the entire growth curve. Bacterial growth was compared to the maternal transposon strain PAO1-4317 using statistical analysis via two-way ANOVA with a Bonferroni post-test,

comparing samples to the control, and determining significance difference for hours 0, 3, 6, 9, and 12. This experiment was repeated 3 times with 4 technical replicates.

2.5 Transposon Mutant Complementation

Genetic complementation of the transposon mutants was performed to assess for restoration of wild type function. The gene was inserted via a plasmid, rather than into the chromosome. This was a lengthened process that required extensive trouble-shooting and multiple steps. The first step was to externally create the DNA to be inserted into the transposon mutants. This insert includes the gene of interest as well as addition of the necessary restriction sites for the gene to be cloned into the vector that would carry it into the mutant cells. A polymerase chain reaction (PCR) is ideal for specific amplification of DNA and allows for large quantities of DNA to be made and for engineered extensions of DNA to be added via elongated primers. PCR primers were designed to amplify the gene of interest and approximately 300-400 base pairs upstream and downstream of the gene (Table 1). In addition, restriction sites were added to the primers for future cloning steps. Restriction sites are used in cloning to perform a site-specific cleave in the DNA with overhangs. These overhang sequences can be bound to similar overhang sequences allowing for gene insertion into a plasmid. Table 1 displays the gene name with the corresponding primer sequences, containing the restriction digest sites (in red). The flanking base pairs (in green) allow for increased efficiency of the restriction digest sites. The expected product size for each PCR product is also displayed on the right-most column and will be used to confirm that the correct PCR product has been formed.

Gene Name	Primer	Primer Sequence	Restriction Enzyme	Expected Product Size (bp)
leuD	forward	CCCGAGCT^CGACCGGGTATTCATCGGTTC	*SacI*	1484
	reverse	CCCA^AGCTTGGGTGGAATAGCGACTGAAGA	*HindIII*	
pfpI	forward	CCGG^AATTCGAAACGGTTGAGGGTGACGA	*EcoRI*	1389
	reverse	CCCA^AGCTTGTTGATGCGATGAACCAGCA	*HindIII*	
moaE	forward	CCGG^AATTCGCCCTGACCATCTACGACAT	*EcoRI*	1308
	reverse	CCCA^AGCTTATGGTGGAAGTGCCGATCTC	*HindIII*	
phnA	forward	CCCGAGCT^CGACTGAGACGGGACATCCAT	*SacI*	1852
	reverse	CCCA^AGCTTCAGCACCAGCAGTTCGCAA	*HindIII*	

Table 1 Forward and reverse primers were designed for each gene to be complemented. The primers contained restriction digest sites to be cleaved (in red), with the ^ representing the exact cut location. Necessary flanking base pairs (in green) were included to increase efficiency of cleavage. The expected length of the PCR product is also shown.

PCR conditions

Many reactants are needed for a PCR, including enzymes, DNA, and cofactors. The Q5® high-fidelity DNA polymerase (New England BioLabs) was used, conferring fidelity of amplification, lower error rates than Taq polymerase, and overall superior performance. The 2x master mix containing the Q5 polymerase also had dNTPs (nucleotide triphosphates), Mg^{2+} cofactor, and Q5 buffer; 25 µL were added to the 50 µL reaction. The forward and reverse primer (Table 1) were resuspended and diluted to 10 µM stocks where 2.5 µL of each primer was added to the reaction. For each sample, 1 µL of genomic PAO1-4317 (wild type) DNA (diluted 1:10) was added into the sample and 19 µL of ultrapure water (Thermo Fischer) topped of the 50 µL. The reaction conditions were 98˚C at 30 s for the initial denaturation step, then 30 cycles of 98˚C denaturation for 10 s, 72˚C annealing for 30 s, and 72˚C extension for 45 s. After 30 cycles, a 72˚C final extension was applied for 2 min allowing for polishing of any unfinished products. The products were confirmed by gel electrophoresis using 1% (10 g/L) agarose dissolved in 1x

TAE (Tris-acetate-EDTA) buffer and the Gene Ruler 1kb DNA Ladder (Thermo Fisher Scientific).

The PCR product was then purified via the PCR Purification Kit (Qiagen). This method used a silica-membrane column to selectively bind the DNA while the undesired salts, primers, enzymes, and other impurities were washed out. Subsequently, the DNA was eluted via 50 µL of ultrapure H_2O, yielding purified DNA that can be used in future reactions.

Restriction digests

The restriction sites used on the primers were chosen based on the restriction sites present on the plasmid, pUCP18 (Figure 3), which served as the vector for transferring genetic material to the mutated cell[23]. The forward and reverse primers were confirmed to not be present within the gene using SnapGene, and were also aligned so that each insert would be in the same orientation within the plasmid, in line with the promoter. The same restriction sites on both the inserts and the plasmid were cut to create overlapping sequences, through staggered restriction enzyme cuts, that were combined in the next step of the complementation process.

The 50-µL digest reaction contained 10 µL of DNA, with the plasmid and insert in separate reactions. The restriction enzyme pair, either EcoRI-hf (high-fidelity) with HindIII-hf or SacI-hf with HindIII-hf, were used based on Table 1 with 1 µL of each added to the reaction. The buffer was decided through the NEBcloner double digest tool, which recommended using the Cutsmart buffer for these combinations of restriction enzymes. Five µL of Cutsmart buffer was added to each reaction and filled to 50 µL with ultrapure H_2O. The digest reaction was incubated at 37˚C for one h and then the restriction enzymes were denatured at 80˚C for 20 min to inactivate them. To confirm that each restriction enzyme was working well, single digests

were also performed and each enzyme was seen to cut the plasmid separately, confirming their proper activity.

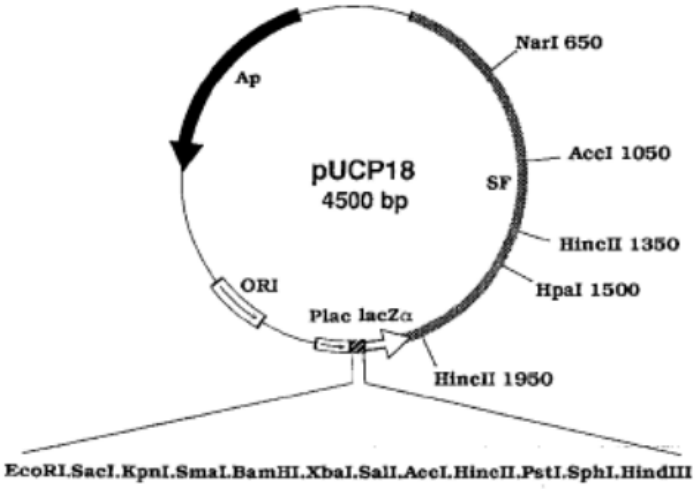

Figure 3 A map of the pUCP18 plasmid displays resistance to ampicillin, part of the *lacZ* gene coding for the first few dozen amino acids of the beta galactosidase enzyme, and various restriction digest sites used for cloning.

Ligation

Each digested insert was mixed with the pUCP18 plasmid, containing the same double digests, and the overlapping regions were ligated to form a single product. The 20 µL ligation experiment called for 2 µL of T4 buffer (NEB), 1 µL of pUCP18, 5 µL of insert, 400 units of T4 DNA ligase enzyme (NEB), and the remaining 20 µL were ultrapure water. The vector and insert were run on the same gel before the experiment and were diluted to the same concentration to be able to control the ratio (1:5) present in the ligation mix. As a control, the ligation was run without the insert to test for ligase effectivity. Another control was running the ligation without the insert or the ligase to test the efficacy of the digest process. The ligations were run at 4˚C overnight and then used for the transformation.

Transformation

The ligation product was introduced into NEB DH5-α competent *E. coli* cells via electroporation. This allows *E. coli* to increase the quantity of the plasmid-insert complex for future transformation back into *P. aeruginosa* transposon mutant cells. Five µL of the ligation mixture were added into a tube containing 50 µL of chilled competent *E. coli* cells. The suspension was incubated on ice for 30 min and then heat shocked at 42˚C for 30 s to induce membrane permeability. The suspension was returned to ice for 2 min and then 950 µL of LB media was added to the suspension to give nutrients to the cell. Cells were grown out for one h shaking at 37˚C and then were plated onto LB agar plates containing ampicillin, IPTG which induces the plasmid, and X-gal. pUCP18 contains ampicillin resistance allowing for selection on ampicillin (100 µg/mL) plates for cells that underwent transformation and acquired the plasmid. Only cells that obtained a copy of the pUCP18 plasmid would be able to survive on ampicillin containing plates. However, there is the possibility that there were cells with copies of pUCP18 that do not contain the gene insert. To screen for these cells, pUCP18 also contains part of the *lacZ* gene, allowing for alpha complementation, which codes for the first few dozen amino acids of beta-galactosidase, an enzyme that cleaves β-galactosides into monosaccharides. The insert is conveniently located to interrupt the function of the *lacZ* gene when inserted into the plasmid. Thus, cells that contain plasmid with an insert will not have functional β-galactosidase enzymes, while cells with plasmids without inserts will have the fully active *lacZ* gene. The plates are coated with a β-galactoside, called X-gal, which is a galactose linked to an indole group, that causes a blue precipitate to appear when it is cleaved. Cells without insert will thus cleave X-gal and will appear as blue colonies on the plate, while cells with pUCP18-insert complexes will

appear as white colonies. White colonies were re-plated onto new Amp100+IPTG+X-gal LB agar plates to confirm the white phenotype.

Confirmation of transposon insert

To confirm that the white colonies did in fact contain the insert, white colonies were grown overnight in LB media. A miniprep plasmid isolation (QIAprep Spin Miniprep Kit by QIAgen) was performed to purify the plasmid from *E. coli* cells. Then the plasmids were once again digested with both restriction enzymes and were electroporated on a gel with the empty pUCP18 plasmid and the PCR products to confirm the presence of the insert.

2.6 Confirming the Presence of the Transposon

As the transposon mutants were used for the biofilm assay experiments, it was important to confirm that the gene was disrupted. The primers used to make the gene inserts can be used to corroborate the interruption of the gene by a transposon. In the wild type strain, the primers bind on either side of the gene and make the approximately 1 kilo base (kb) product for each of the samples tested. However, since the transposon insert is many kb long and inserts within the gene, the primers will be amplifying a different sequence for the transposon mutants. The bases between the primers increases by many kb and becomes too long to be amplified in the short extension time present for the PCR. Consequently, if the transposon is present in the mutant, a product should not form and no band would show up on the gel electrophoresis. This is run adjacent to the PCR product, using PAO1 as the template DNA, rather than the mutant strains. All of the conditions are the same for both PCR reactions except for the genomic DNA, ensuring differences would be a consequence of the transposon being present.

3. Results

3.1 RNAseq Detected 437 Candidate Genes Potentially Implicated in Biofilms (work conducted by Christopher Jones, Ph.D.)

We analyzed the RNAseq results and identified 437 candidate genes that were potentially implicated in playing a role in bacterial surface attachment. These genes were identified by differential expression analysis using Rockhopper. Differential gene expression was observed between 5-60 min after attachment, with the peak mRNA expression at 30 min post-attachment (Figure 4), and this time point was used to show initial bacterial response to a surface. The genes expressed after 30 min were compared to gene expression at 5 min, where mRNA differential expression had not yet begun, appearing as planktonic profiling. Statistically significant differentially accumulated mRNAs were parsed to include only those with a 1.7-fold change (Supplemental Table 1). As expected, genes in the same operon were seen to have regulation with similar trends, supporting the validity of the transcriptomic study (Table 2).

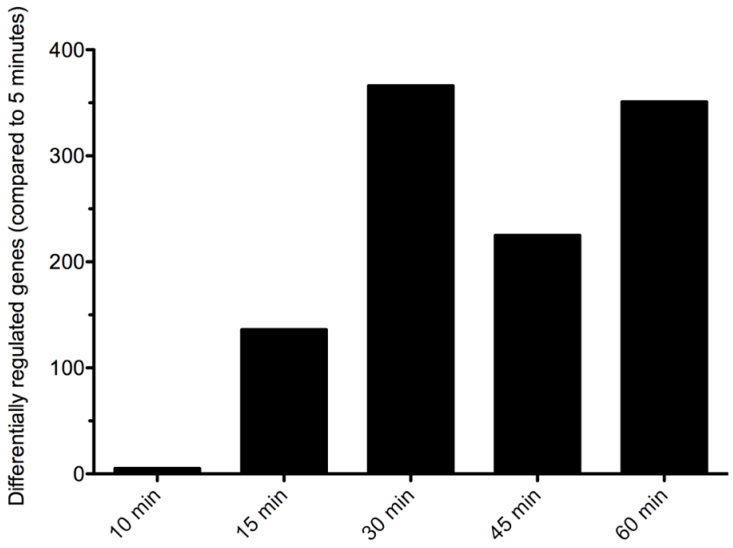

Figure 4 mRNA accumulation analysis identified the peak response to bacterial surface attachment occurring at 30 minutes, as compared to the 5-minute attachment time point. These genes were analyzed for mRNA accumulation fold-changes in comparison to planktonic cells.

Mutant gene	Genes involved in operon		
phnA operon	*phnA* (PA1001)	*phnB* (PA1002)	
leuD operon	*leuD* (PA3120)	*leuC* (PA3121)	
pfpI operon	*pfpI* (PA0355)		
moaE operon	*moaE* (PA3916)	*moaD* (PA3917)	*moaC* (PA3918)

Table 2 The RNAseq data also confirms that operons are being coordinately expressed. Red represents reduced mRNA and green represents elevated mRNA levels compared to the 5-minute control.

3.2 Confirmation of Transposon Mutants

When using transposon mutant libraries, there is always the possibility that the gene labeled was not disrupted and that the function of the strain is normal. To confirm that the transposon had inserted where the catalog mentioned it would, the primers that were designed for the complementation process were used. The primer pairs amplified the gene region of the PAO1 strain and the transposon mutant strains and the results were compared. The size of the product using the genomic DNA template of the PAO1 yielded the expected sizes for the gene and a few hundred base pairs on each side (Figure 5). In comparison, the genomic DNA template of the transposon mutants was seen to not yield any PCR product (Figure 5). This is a result of the transposon inserting within the region to be amplified and increasing the size of this region in the genomic DNA by many kilobases. Increasing distance between the primer pairs causes a failure in producing the PCR product. This result confirms the presence of a transposon mutant in each of the 4 mutant strains in the location of the specified gene.

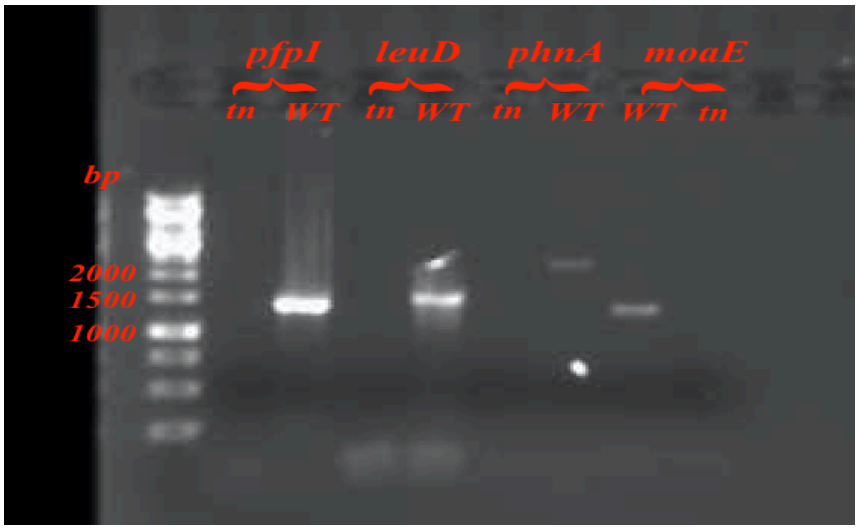

Figure 5 Primer pairs amplified the region around where each gene should be yielding the insert product for the PAO1 (WT) genomic DNA. The transposon (Tn) mutants had large inserts that prevented the PCR product from forming, illustrating the presence of the transposon disruption in the mutants.

3.3 Biofilm Assays Reveal Disrupted Biofilm Mutants

The transposon mutants from the 30 most elevated and the 8 most reduced genes were tested for biofilm formation using biofilm rapid attachment assays with crystal violet staining. Biofilm formation was normalized to PAO1 and compared to PAO1Δ*psl*, a mutant with decreased biofilm capacity[24], and PAO1Δ*wspF*, a mutant with enhanced biofilm characteristics[25]. After 3 h of growth at 37˚C, the bacterial strains harboring mutations in the 30 most upregulated genes showed decreased biofilm levels in 13 transposon mutants (Figure 6A). From the bacterial strains with mutations in the 8 most downregulated genes, 5 transposon mutants showed decreased biofilm levels with a confidence interval of $p \leq 0.05$ (Figure 6B). Although mutants in PA0509, PA0499, PA1930, PA3337, PA0324, PA4889, PA2969, and PA0994 showed average biofilm accumulation higher than PAO1, there was no statistical difference from the wild type. Because of their reproducible decrease in biofilm formation over several experiments, four mutants, *leuD*::IS*lacZ*/hah, *phnA*::IS*phoA*/hah, *pfpI*::IS*phoA*/hah, and *moaE*::IS*phoA*/hah were

selected for complementation and further analysis. After normalization, these mutants had significantly reduced biofilm levels: *leuD*::IS*lacZ*/hah (PA3120) had an average of 0.2027 (±0.1020), *phnA*::IS*phoA*/hah (PA1001) averaged 0.2028 (±0.1419), *pfpI*::IS*phoA*/hah (PA0355) averaged 0.7066 (±0.2045), and *moaE*::IS*phoA*/hah (PA3916) averaged 0.7099 (±0.1578). For the *phnA* and *leuD* mutants, levels of biofilm were comparable to Δ*psl*.

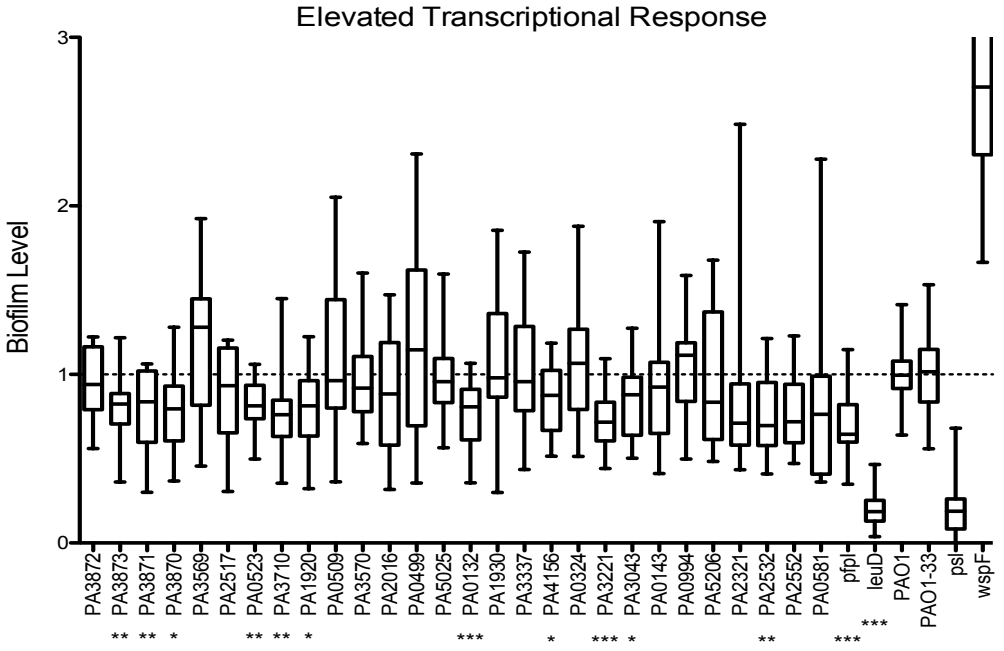

A

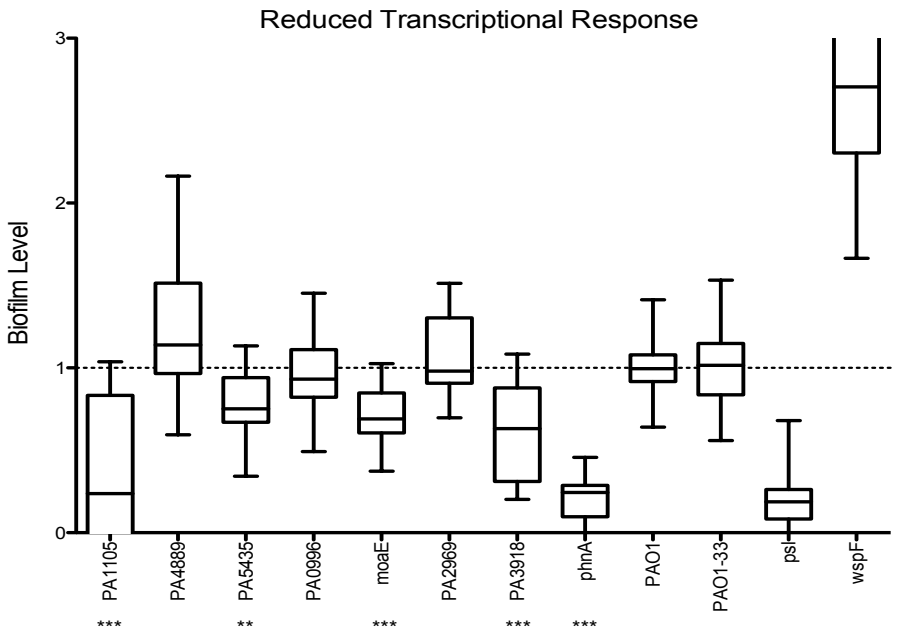

B

Figure 6 A-B. Transposon insertions in surface-regulated genes were seen to affect bacterial attachment to surfaces. Biofilm assays were performed in quadruplicate on transposon mutants of each strain harboring a mutation in a non-essential surface-regulated gene. The results from the mutants corresponding to disruptions in the genes with the (A) 30 highest and (B) 8 lowest mRNA accumulation changes are presented here in box-and-whisker plots. The dotted horizontal line at 1 indicates the relative attachment of PAO1-4317. *= $P \leq 0.05$, **= $P \leq 0.01$, ***= $P \leq 0.001$.

3.4 Analysis of Mutant Growth Rates

When comparing levels of biofilm formation, there is a possibility that differences in growth rate rather than attachment strength are responsible for the different biofilm levels. To test for this possibility, transposon mutants *leuD*::IS*lacZ*/hah, *phnA*::IS*phoA*/hah, *pfpI*::IS*phoA*/hah, and *moaE*::IS*phoA*/hah growth rates were compared to the wild type (PAO1-4317). Growth was measured over a 22-hour period at 37˚C in LB media, with only the first 12 hours shown as this is where the maximum OD_{600} was achieved and the samples plateaued afterwards. Statistical analysis was performed at 0, 3, 6, 9, and 12 hours of growth comparing to PAO1 wild type. The mutants *leuD*::IS*lacZ*/hah and *phnA*::IS*phoA*/hah appeared to have reduced

growth rate over the first 3 and 6 hours (Figure 7), however by 9 and 12 hours the OD_{600} seemed to level with the wild type strain.

Inversely, *pfpI*::IS*phoA*/hah and *moaE*::IS*phoA*/hah exhibited higher OD_{600} values throughout the entire growth curve experiment (Figure 7), suggesting that the disruption of gene *pfpI* and *moaE* acted antagonistically with biofilm formation. This depressed level of biofilm remained present even as the OD_{600} of the mutant strains increased to the levels of PAO1.

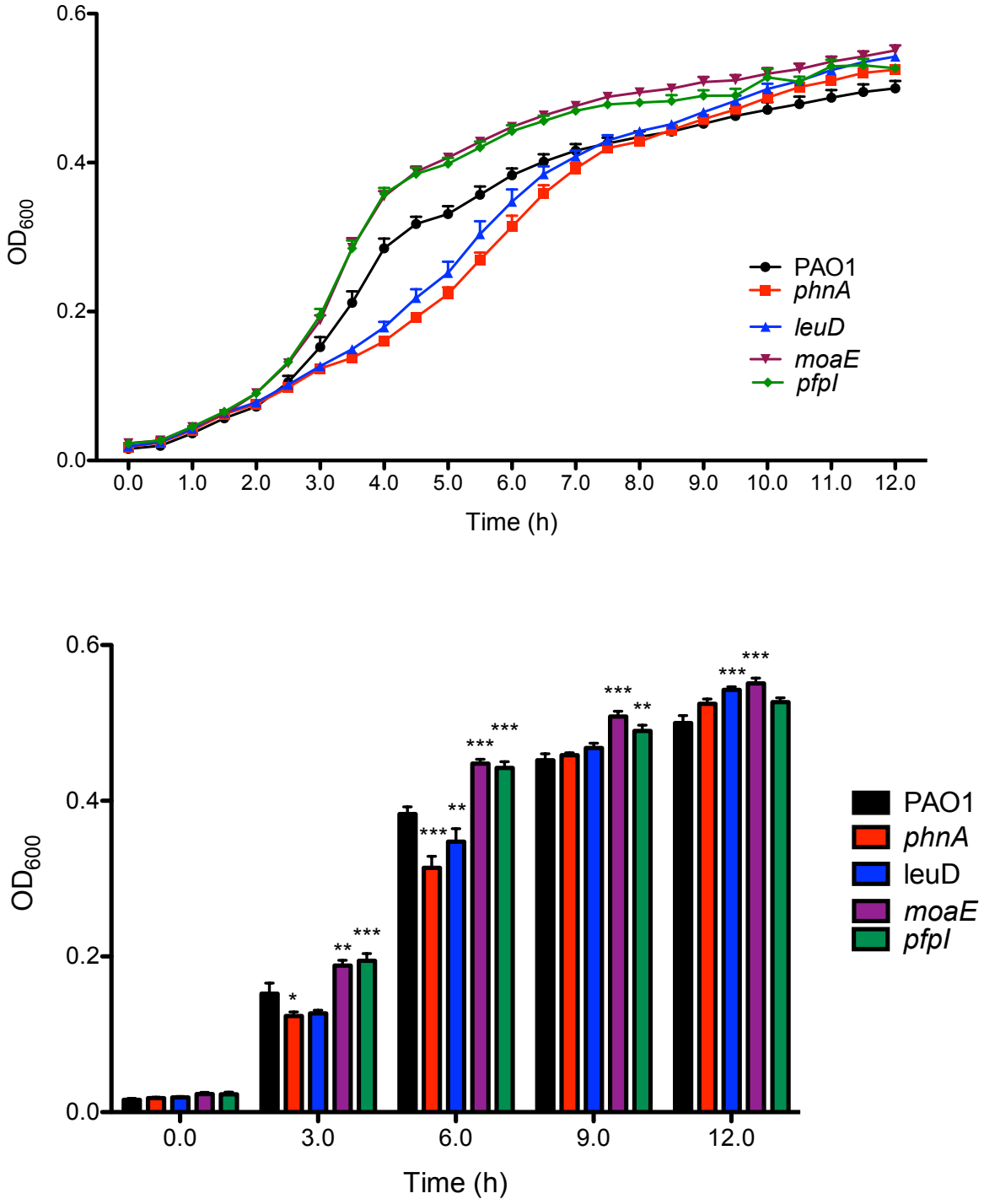

Figure 7 Growth curves in LB media showed the *moaE* and *pfpI* transposon mutants had elevated growth over the course of the 12 hours. Whereas, *phnA* and *leuD* had slower growth for the first 6 hours and then became similar to the PAO1-4317 wild type. Statistical analysis shows the slight differences in OD_{600} between samples throughout the growth curves.

3.5 Minimal Media Displayed Similar Growth to Nutrient Rich Media

Since many of the mutants were involved in metabolic pathways, growth on Vogel-Bonner minimal medium was observed. VBMM mirrored LB growth curves with similar optical densities reached, peaking at around OD_{600}=0.6. When compared to the wild type growth curve, *leuD*::IS*lacZ*/hah and *phnA*::IS*phoA*/hah again have lower growth after 3 hours but surpass wild type growth by 9 and 12 hours (Figure 8),. *pfpI*::IS*phoA*/hah and *moaE*::IS*phoA*/hah have higher growth throughout the experiment after 3 hours, similar to the LB media trends. The minimal media did not have any major adverse effects on growth for either the wild type or the mutants tested.

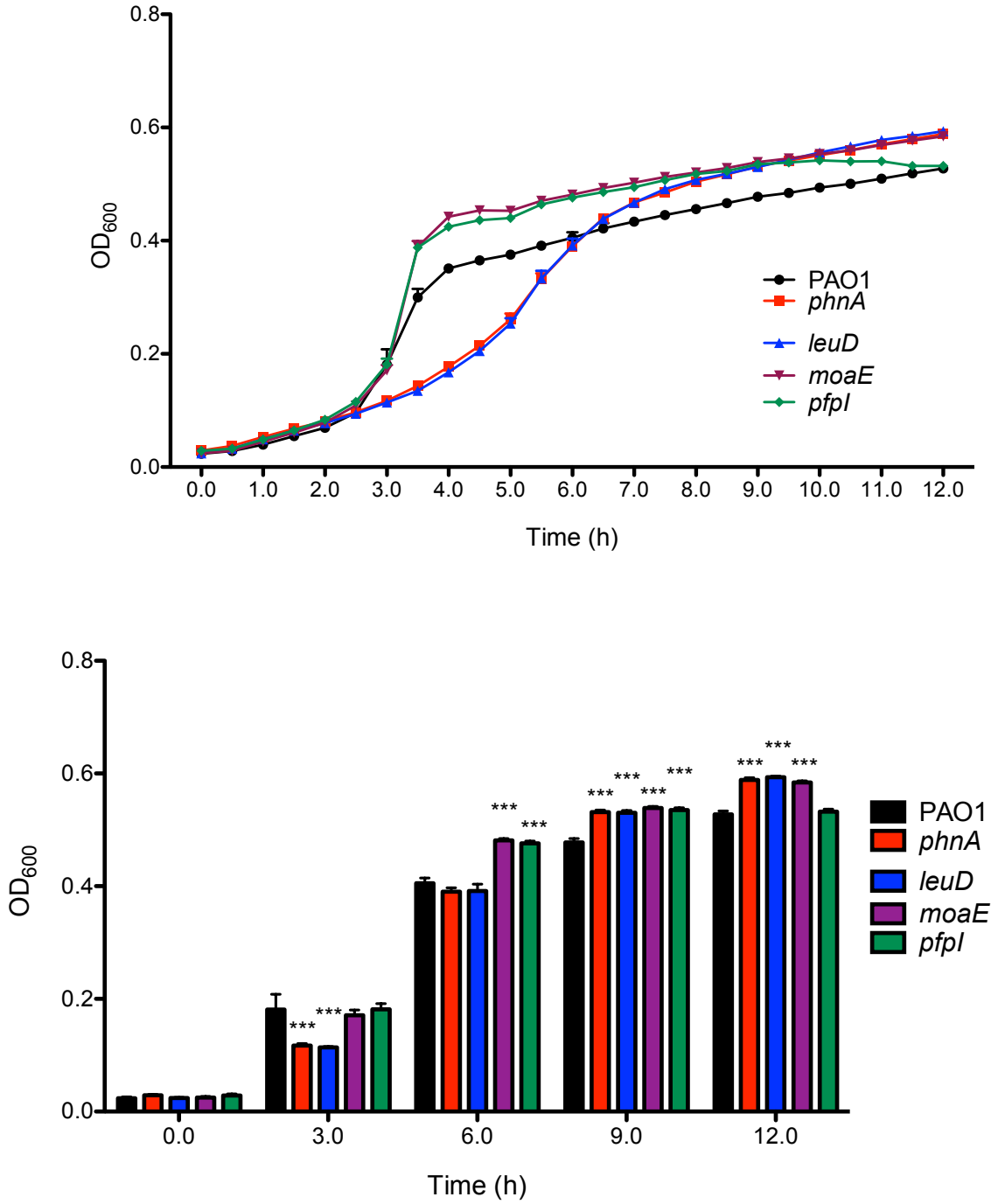

Figure 8 Growth curves in VBMM also showed elevated growth in the *moaE* and *pfpI* transposon mutants after the 3-h time point. *phnA* and *leuD* had slower growth for only the first 3 hours and then became level and surpassed the PAO1 wild type. Three-h intervals are compared with statistical analysis showing slight differences in growth between samples. *= $P \leq 0.05$, **= $P \leq 0.01$, ***= $P \leq 0.001$.

3.6 Lengthened Rapid Attachment Assays Show Biofilm Disruption

The reduced growth rate of *leuD*::IS*lacZ*/hah and *phnA*::IS*phoA*/hah until hour 6 of the growth curves suggest that biofilm levels could be increasing for these samples with respect to PAO1 with a longer incubation time on the biofilm assay, as the optical density equalizes. However, when the incubation time is increased to 6 h, the biofilm level of *leuD*::IS*lacZ*/hah and *phnA*::IS*phoA*/hah is seen to remain well below the biofilm level of PAO1 (Figure 9 A-B). At 6 h of attachment time, *leuD*::IS*lacZ*/hah exhibits an average of 0.1698 (±0.0321) compared to its 3-h average of 0.2027 (±0.1020); at 6 h of biofilm growth *phnA*::IS*phoA*/hah has a normalized average of 0.2154 (±0.0185) compared to its 3-h average of 0.2028 (±0.1419) (table 2). In both cases, the change in biofilm level after three hours is minimal and does not indicate a positive correlation with optical density to the degree that would be expected in a wild-type biofilm formation. Together, these observations indicate that the reduced biofilm phenotype of these transposon mutants is independent of growth rate, implicating *leuD, phnA*, *moaE* and *pfpI* as novel genes important for biofilm formation in *P. aeruginosa.*

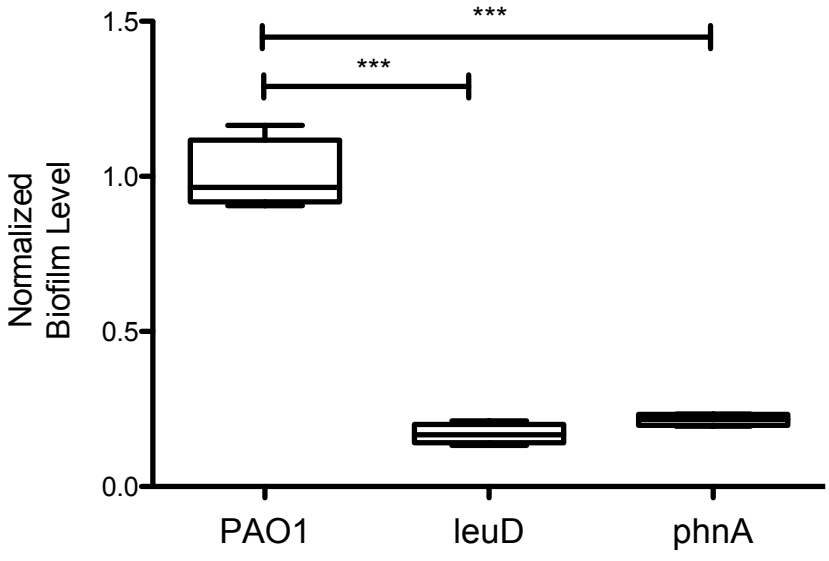

A

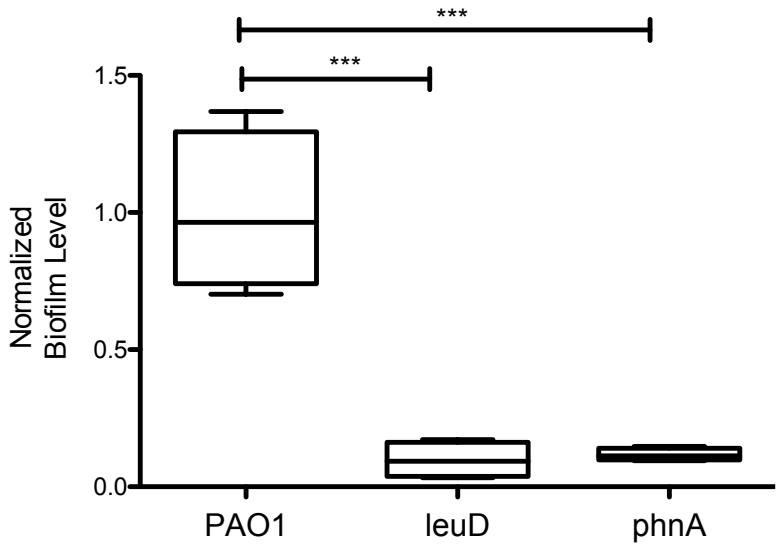

B

Figure 9 A-B An increase in optical density did not result in an increase in biofilm level after 6 h of attachment for *leuD* or *phnA* in either LB media (A) or VBMM (B). Growth was compared in both media to adjust for the slightly different growth pattern. The level of biofilm for both mutants is significantly lower than in the wild type PAO1 strain in both media. Three and six hour biofilms are compared in Table 2. ***= $P \leq 0.001$.

	3-hour		6-hour	
Sample	Rel. OD_{600}	Normalized biofilm level	Rel. OD_{600}	Normalized biofilm level
PAO1-4317	0.1522	1	0.3831	1
phnA	0.1235	0.2028	0.3138	0.2154
leuD	0.1268	0.2027	0.3476	0.1698

Table 2 Results from Figures 6, 7 and 9A are combined to compare the OD_{600} of PAO1-4317 and the slightly slower growth of *phnA*::IS*phoA*/hah and *leuD*::IS*lacZ*/hah to the sustained decreased level of biofilm present. This data does not show a growth defect reason for the substantial difference in biofilm level displayed. The difference in biofilm level is due to factors that are not related to the number of cells present.

3.7 Complementation of Transposon Mutants

When a transposon disrupts a gene, there is the possibility that there will be additional effects downstream in the same operon. These are called polar effects and are quite common if

the disruption of a gene upstream interrupts the transcript and prevents transcription of the entire mRNA coded by the operon. When genes downstream are not transcribed, it becomes unclear whether phenotypic variations are caused by the gene disrupted or by ones downstream. To address this problem, the gene of interest is re-inserted into the transposon mutant to restore wild-type function to the mutant. The process of engineering the mutant to once again contain the gene is called complementation. The complement constructs were successfully made but delays were encountered due to the epidemic in performing the final complementation experiments. These final experiments include re-assessing the complemented strains to determine if biofilm formation has been restored to wild-type levels. This would support claims that the gene that has been disrupted was the one responsible for the vast changes seen in biofilm level.

4. Discussion

It was posited that genes regulated upon surface contact play a role in sensing the surface and assisting in the transition from a motile to sessile lifestyle. To test this hypothesis, various time points of bacterial attachment were compared to the planktonic cells and *P. aeruginosa* was seen to have the greatest mRNA response at 30 min post-attachment. The genes that were differentially expressed at this time point were compared and classified by fold-change and statistical significance of differential mRNA accumulation. Subsequent rapid attachment assays were performed on the top 38 mutants with differential mRNA levels at 30 min post-attachment. These genes were selected due to their elevation and reduction in transcriptional response, suggesting a participation in the bacterial attachment process. Support for the validity of the

transcriptional study stems from genes present in the same operon that were observed to be differentially expressed in the same direction.

Although transcriptional responses showed large levels of elevation and reduction across these 38 genes, differences in attachment of the corresponding mutant lines compared to the wild type strain, studied through crystal violet assays, were seen in only 18 of these genes. All the biofilm levels that were significantly different appeared to be decreasing the level of biofilm in comparison to the wild type. Transposon inserts were corroborated by comparing wild-type genomic DNA to mutant genomic DNA at the location of the genes of interest. These samples were compared via PCR and the transposon insertion appeared to be present in each mutant.

As with any transposon mutant, there are caveats that apply. Specifically, there may be polar effects retained by some of the mutants that affect the expression of a gene that is present downstream. To overcome these limitations, complementation assays are being carried out to identify the effect of restoring the gene to the transposon mutant. Despite, these caveats, functional testing of the biofilm capabilities of these strains was determined to be the most efficient screen to identify genes that are involved in surface attachment and biofilm formation. To confirm attachment changes, biofilm rapid attachment assays were performed on 38 mutants, displaying highest and lowest mRNA expression, and were repeated four times. These assays confirmed that a subset of surface-regulated genes is reproducibly involved in surface attachment and biofilm initiation (Supplemental Figure 1).

Further analysis on the *leuD*::IS*lacZ*/hah, *phnA*::IS*phoA*/hah, *pfpI*::IS*phoA*/hah, and *moaE*::IS*phoA*/hah samples showed reduced surface attachment compared to PAO1. Expression of *leuD* and *pfpI* was elevated upon surface attachment and interruption with a transposon reduced biofilm initiation, suggesting the products of these genes are beneficial for bacterial

attachment. Inversely, *phnA* and *moaE* had lower mRNA expression upon 30 min post attachment. An explanation for the knockout of a lower expressed gene causing a decrease in biofilm levels could be that the cells are playing a role in cell-cell interactions rather than actual cellular attachment to the surface. These gene would be expressed less in the initial attachment phase of the biofilm but would be expressed more after intercellular interactions begin to occur. Thus, the disruption of *pnhA* and *moaE* would decrease biofilm levels through inhibiting bacterial interactions rather than surface-cell attachment.

The *pfpI* gene codes for the PfpI protease and serves as a general anti-stress response gene. The *pfpI* gene has been seen to provide protection to *P. aeruginosa* against UV radiation, salt, heat, and confers DNA protection under normal conditions[26]. Even though the *pfpI* mutant has been previously implicated in biofilms, it is unknown how PfpI activity leads to biofilm formation. Biofilm development facilitates growth for bacteria and shields cells from environmental toxins and hazards. It is possible that given the role *pfpI* plays in stress response that it also assists in controlling biofilm formation to afford additional cellular protection. Removal of this gene would then jeopardize biofilm formation and cause disruption of a biofilm related pathway.

The *moaE* gene codes for the large subunit of the molybdopterin converting factor (*Pseudomonas* Genome DB). Molybdopterins are cofactors coordinating molybdenum and tungsten in enzymes.[27] This molybdenum cofactor (Moco) is an essential portion of proteins including DMSO reductase, sulfite oxidase, nitrate reductase, and xanthine oxidase involved in the cellular respiration through the sulfur, nitrogen, and carbon cycles[28]. The inability to properly form these enzymes could be having ramifications on availability of nutrients to produce exopolysaccharides, adhesins, and other factors that assist in bacterial attachment and biofilm

formation. Since *moaE* had reduced mRNA levels at early levels of biofilm attachment, it could be serving as a precursor to production of intercellular communication molecules. The *moaE* would then have difficulty in producing robust biofilms through decreases in cellular aggregation.

The *leuD* gene codes for the small subunit of 3-isopropylmalate dehydratase (*Pseudomonas* Genome DB), an important sub pathway that synthesizes L-leucine. With a reduction of leucine in the cells, the bacteria would conserve this nutrient for essential growth. There is, however, a leucine aminopeptidase that is overly expressed in biofilm formation as it forms virulent outer membrane vesicles[29]. Without leucine production occurring in the cell, there would be a decrease in the amount of outer membrane vesicles produced leading to a decrease in cellular virulence and biofilm formation.

The *phnA* gene codes for the anthranilate synthase component I (*Pseudomonas* Genome DB), an enzyme that catalyzes the bidirectional reaction of anthranilate, pyruvate, and glutamate from chorismate and L-glutamine[30]. Anthranilate inhibits formation of biofilms by a number of bacteria including *P. aeruginosa, Vibrio vulnificus,* and *Bacillus subtilis* by reducing swimming and swarming motilities necessary for aggregation[31]. However, another study noted that biofilm formation was assisted by basal levels of the anthranilate degradation pathway[32]. This presents two theories for why the disruption of the *phnA* gene would disrupt biofilm levels. There is a possibility that anthranilate is building up preventing biofilm formation due to its toxic effect. Concurrently, it is possible that the interruption of the anthranilate degradation pathway is also lowering biofilm production levels.

In addition to the genes selected for further study, there are also many encoding hypothetical proteins. We expect future work and analysis will elucidate the functions of these genes, resulting in a more complete understanding of how they affect biofilm formation.

P. aeruginosa and other bacteria with a wide range of niches attach to many different surfaces as they transition from one environment to another. The surfaces that are colonized span from soil particles to lung epithelium, with a vast disparity in the physical and chemical properties, as well as the stressors that must be overcome to establish a biofilm. For aggregation and formation of a biofilm community to occur, the bacteria must sense, respond, and bind specifically to each surface. It has been demonstrated that stiffness of a surface material affects bacterial attachment, biofilm formation, and intracellular signaling[33]. Proteomic studies of biofilms formed on abiotic surfaces found that there were specific responses to various surfaces, with 70 proteins varying in level of detection between different surfaces[34]. The literature indicated that members of the proteomes were specifically regulated on different surfaces. hypothesized that bacteria sense various materials and initiate a unique response to each surface. In this study, bacterial responses were determined by performing RNA-seq on adherent bacterial populations at 30 minutes after attachment. We demonstrated that there are unique transcriptional responses to three different abiotic surfaces, with minimal shared transcriptional responses (Supplemental Figure 2). We used transcriptional regulation to show that *P. aeruginosa* exhibits a unique response to specific surfaces (Supplemental Figure 2) rather than a more generalized response with a few specific novel genes regulated. Few genes were regulated in a similar fashion among the different surfaces, suggesting the bacteria had a nearly unique transcriptional response to specific surfaces, with minimal overlap. Although completely unique responses to each surface were unexpected, the transcriptional profiles suggest that the bacteria

can sense and react to different surfaces via a unique transcriptional cascade that seems to occur within the first 30 minutes of attachment (Figure 4).

This study demonstrates that *P. aeruginosa* elicits a rapid and specific transcriptional response to various abiotic surfaces resulting in bacterial attachment and biofilm initiation. From the few genes that were conserved across different surfaces, it is clear that *P. aeruginosa* is able to sense, not only an encounter with a surface, but also to fine tune their responses to certain properties present on each surface. Differences on surfaces may include chemical composition, hardness, viscosity, hydrophobicity, or texture. My results do not precisely elucidate what the bacteria are sensing, however, future work could examine the mechanisms of surface sensing and signaling that are resulting in the drastically different responses to abiotic surface attachment.

These results raise the intriguing possibility of selecting materials in health-care settings based on reduced levels of colonization properties. Other options include engineering surfaces that resist colonization of opportunistic pathogens by preventing surface recognition and interactions of bacteria. Due to the present increased spread of antimicrobial resistance and the tenacity of biofilms to survive antibiotics, it is essential to investigate novel approaches to sanitation, infection control, and limitation of biofilm formation. We propose that these studies present a stepping stone for understanding the initial stages of biofilm formation that may be exploited in future developments of bacterial control strategies.

Supplemental Figures

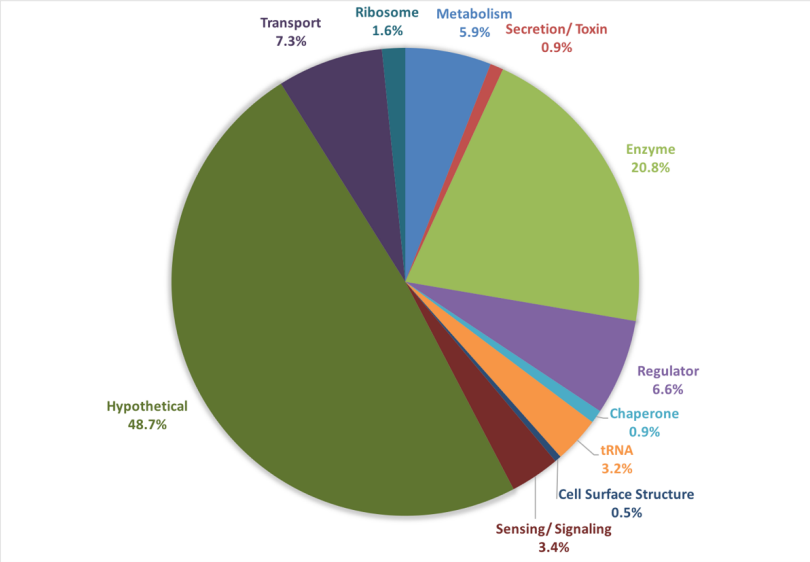

Supplemental Figure 1 Categorization of the known functions of the various genes that were seen to be differentially expressed in the study. With the majority being hypothetical proteins and others being potentially involved in surface sensing and shifting the bacteria from a planktonic lifestyle to an aggregated colony.

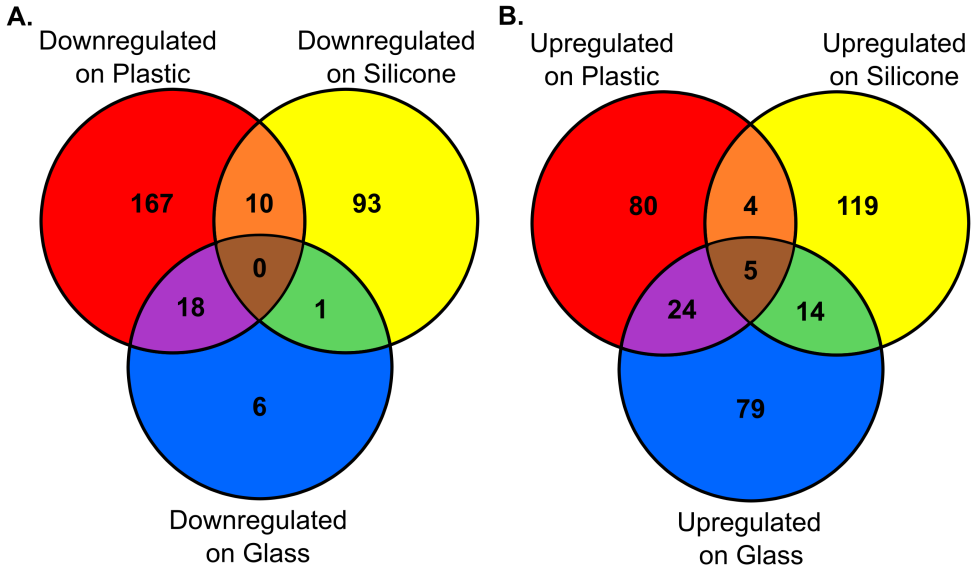

Supplemental Figure 2 There is a unique transcriptional response present to each surface *P. aeruginosa* attaches to, showing the low number of conserved genes in the attachment response. The bacteria sense unique surfaces differentially and exhibit distinct responses to plastic, glass, and silicone.

PA number	Name	Description of the Putative Gene Product	Fold Change	qValue 5 min vs 30 min
PA3872	narI	respiratory nitrate reductase subunit gamma	12.1	3.2E-189
PA3873	narJ	respiratory nitrate reductase subunit delta	8.0	1.8E-73
PA3871	-	PpiC-type peptidyl-prolyl cis-trans isomerase	7.7	4.0E-61
PA3870	moaA1	molybdenum cofactor biosynthesis protein A	7.3	1.9E-58
PA3569	mmsB	3-hydroxyisobutyrate dehydrogenase	7.0	1.3E-40
PA2517	xylY	toluate 1,2-dioxygenase subunit beta	6.2	1.8E-34
PA0523	norC	nitric-oxide reductase subunit C	5.9	2.0E-07
PA3710	-	GMC-type oxidoreductase	5.0	7.3E-24
PA1920	nrdD	anaerobic ribonucleoside triphosphate reductase	5.0	3.5E-22
PA0509	nirN	cytochrome C	5.0	1.1E-18
PA3570	mmsA	methylmalonate-semialdehyde dehydrogenase	4.5	3.2E-17
PA2016	liuR	regulator of liu genes	4.4	2.9E-09
PA0499	-	pili assembly chaperone	4.3	6.1E-18
PA5025	metY	O-acetylhomoserine aminocarboxypropyltransferase	4.2	1.3E-11
PA0132	-	beta alanine--pyruvate transaminase	4.2	2.0E-14
PA1930	-	chemotaxis transducer	4.1	3.8E-15
PA3337	rfaD	ADP-L-glycero-D-manno-heptose-6-epimerase	3.9	1.1E-07
PA4156	-	TonB-dependent receptor	3.9	2.1E-11
PA0324	-	ABC transporter permease	3.9	1.9E-13
PA3221	csaA	CsaA protein	1.8	2.9E-02
PA3043	-	deoxyguanosinetriphosphate triphosphohydrolase-like protein	1.8	3.3E-02
PA0143	nuh	nonspecific ribonucleoside hydrolase	1.8	3.1E-02
PA0994	cupC3	usher CupC3	1.8	3.1E-02
PA5206	argE	acetylornithine deacetylase	1.8	3.3E-02
PA2321	-	gluconokinase	1.8	2.9E-02
PA2532	tpx	thiol peroxidase	1.8	3.6E-02
PA2552	-	acyl-CoA dehydrogenase	1.8	3.6E-02
PA0581	-	glycerol-3-phosphate acyltransferase PlsY	1.8	3.4E-02
PA0355	pfpI	protease PfpI	1.7	3.1E-02
PA3120	leuD	isopropylmalate isomerase small subunit	1.7	3.3E-02

PA number	Name	Description of the Putative Gene Product	Fold Change	qValue 5 min vs 30 min
PA1105	fliJ	flagellar biosynthesis chaperone	0.38	3.9E-02
PA4889	-	oxidoreductase	0.37	4.4E-02
PA5435	-	pyruvate carboxylase subunit B	0.34	4.4E-02
PA0996	pqsA	coenzyme A ligase	0.34	1.9E-02
PA3916	moaE	molybdopterin converting factor large subunit	0.33	3.2E-02
PA2969	plsX	glycerol-3-phosphate acyltransferase PlsX	0.31	2.0E-02
PA3918	moaC	molybdenum cofactor biosynthesis protein MoaC	0.30	1.9E-02
PA1001	phnA	anthranilate synthase component I	0.26	1.3E-04

Supplemental Table 1 All the samples that underwent biofilm crystal violet testing are shown with the gene name, the putative gene product, and the fold change seen in the RNAseq. The RNAseq attachment assay was run on a polymer surface.

References

[1] Revelas, A. (2012). Healthcare - associated infections: A public health problem. Nigerian Medical Journal, 53(2), 59. doi: 10.4103/0300-1652.103543

[2] Glance, L. G. (2011). Increases in Mortality, Length of Stay, and Cost Associated With Hospital-Acquired Infections in Trauma Patients. Archives of Surgery, 146(7), 794. doi: 10.1001/archsurg.2011.41

[3] Stephanie J. Cole, Angela R. Records, Mona W. Orr, Sara B. Linden, Vincent T. Lee Infection and Immunity Apr 2014, 82 (5) 2048-2058; DOI: 10.1128/IAI.01652-14

[4] Gestel, J. V., Vlamakis, H., & Kolter, R. (2015). Division of Labor in Biofilms: the Ecology of Cell Differentiation. Microbial Biofilms, 67–97. doi: 10.1128/9781555817466.ch4

[5] Donlan, R. M., & Costerton, J. W. (2002). Biofilms: Survival Mechanisms of Clinically Relevant Microorganisms. Clinical Microbiology Reviews, 15(2), 167–193. doi: 10.1128/cmr.15.2.167-193.2002

[6] Rasmussen, T. B., & Givskov, M. (2006). Quorum-sensing inhibitors as anti-pathogenic drugs. International Journal of Medical Microbiology, 296(2-3), 149–161. doi: 10.1016/j.ijmm.2006.02.005

[7] Most Common Healthcare-Associated Infections: 25 Bacteria, Viruses Causing HAIs. (2014, May 1). Retrieved from https://www.beckershospitalreview.com/quality/most-common-healthcare-associated-infections-25-bacteria-viruses-causing-hais.html

[8] Gil-Perotin, S., Ramirez, P., Marti, V., Sahuquillo, J. M., Gonzalez, E., Calleja, I., … Bonastre, J. (2012). Implications of endotracheal tube biofilm in ventilator-associated pneumonia response: a state of concept. Critical Care, 16(3). doi: 10.1186/cc11357

[9] Brüssow, H. (2012). Pseudomonas Biofilms, Cystic Fibrosis, and Phage: a Silver Lining? MBio, 3(2). doi: 10.1128/mbio.00061-12

[10] Delden, C. V., & Iglewski, B. H. (1998). Cell-to-cell signaling and Pseudomonas aeruginosa infections. Emerging Infectious Diseases, 4(4), 551–560. doi: 10.3201/eid0404.980405

[11] E. Maunders and M. Welch, "Matrix exopolysaccharides; the sticky side of biofilm formation," FEMS Microbiol. Lett., vol. 364, no. 13, pp. 1–10, 2017.

[12] Czaczyk, K., & Myszka, K. (2007). Biosynthesis of Extracellular Polymeric Substances (EPS) and Its Role in Microbial Biofilm Formation. Polish Journal of Environmental Studies, 16(6), 799–806.

[13] Lee, K., & Yoon, S. S. (2017). Pseudomonas aeruginosa Biofilm, a Programmed Bacterial Life for Fitness. Journal of Microbiology and Biotechnology, 27(6), 1053–1064. doi: 10.4014/jmb.1611.11056

[14] Whiteley, M., Bangera, M. G., Bumgarner, R. E., Parsek, M. R., Teitzel, G. M., Lory, S., & Greenberg, E. P. (2001). Gene expression in Pseudomonas aeruginosa biofilms. Nature, 413(6858), 860–864. doi: 10.1038/35101627

[15] Moorthy, S., & Watnick, P. I. (2005). Identification of novel stage-specific genetic requirements through whole genome transcription profiling ofVibrio cholerae biofilm development. Molecular Microbiology, 57(6), 1623–1635. doi: 10.1111/j.1365-2958.2005.04797.x

[16] Mikkelsen, H., Ball, G., Giraud, C., & Filloux, A. (2009). Expression of Pseudomonas aeruginosa CupD Fimbrial Genes Is Antagonistically Controlled by RcsB and the EAL-Containing PvrR Response Regulators. PLoS ONE, 4(6). doi: 10.1371/journal.pone.0006018

[17] Williamson, W. M., Close, M. E., Leonard, M. M., Webber, J. B., & Lin, S. (2012). Groundwater Biofilm Dynamics Grown In Situ Along a Nutrient Gradient. Ground Water, 50(5), 690–703. doi: 10.1111/j.1745-6584.2011.00904.x
[18] Wyckoff, T. J., & Wozniak, D. J. (2001). [14] Transcriptional analysis of genes involved in pseudomonas aeruginosa biofilms. Methods in Enzymology Microbial Growth in Biofilms - Part A: Developmental and Molecular Biological Aspects, 144–151. doi: 10.1016/s0076-6879(01)36586-2
[19] Kang, D., & Kirienko, N. V. (2017). High-Throughput Genetic Screen Reveals that Early Attachment and Biofilm Formation Are Necessary for Full Pyoverdine Production by Pseudomonas aeruginosa. Frontiers in Microbiology, 8. doi: 10.3389/fmicb.2017.01707
[20] Costerton, J. W., & Lappin-Scott, H. (1995). Introduction to Microbial Biofilms. Microbial Biofilms, 1–12. doi: 10.1017/cbo9780511525353.002
[21] Dr. Christopher Jones was a postdoctoral researcher in Dr. Daniel Wozniak's laboratory
[22] Jacobs, M. A., Alwood, A., Thaipisuttikul, I., Spencer, D., Haugen, E., Ernst, S., … Manoil, C. (2003). Comprehensive transposon mutant library of Pseudomonas aeruginosa. Proceedings of the National Academy of Sciences, 100(24), 14339–14344. doi: 10.1073/pnas.2036282100
[23] Schweizer, H. (1991). Escherichia-Pseudomonas shuttle vectors derived from pUC18/19. Gene, 97(1), 109–112. doi: 10.1016/0378-1119(91)90016-5
[24] Jones, C. J., & Wozniak, D. J. (2017). Psl Produced by Mucoid Pseudomonas aeruginosa Contributes to the Establishment of Biofilms and Immune Evasion. MBio, 8(3). doi: 10.1128/mbio.00864-17
[25] Ryder, C., Byrd, M., & Wozniak, D. J. (2007). Role of polysaccharides in Pseudomonas aeruginosa biofilm development. Current opinion in microbiology, 10(6), 644–648. https://doi.org/10.1016/j.mib.2007.09.010
[26] Rodríguez-Rojas Alexandro, & Blázquez Jesús. (2000). The Pseudomonas aeruginosa pfpI Gene Plays an Antimutator Role and Provides General Stress Protection. Journal of Bacteriology, 191(3), 844–850. doi: 10.1128/jb.01081-08
[27] Daniels, J. N., Wuebbens, M. M., Rajagopalan, K. V., & Schindelin, H. (2008). Crystal Structure of a Molybdopterin Synthase−Precursor Z Complex: Insight into Its Sulfur Transfer Mechanism and Its Role in Molybdenum Cofactor Deficiency. Biochemistry, 47(2), 615–626. doi: 10.1021/bi701734g
[28] Hille, R. (1996) The Mononuclear Molybdenum Enzymes, Chem. Rev.96, 2757−2816.
[29] Esoda, C. N., & Kuehn, M. J. (2019). Pseudomonas aeruginosa Leucine Aminopeptidase Influences Early Biofilm Composition and Structure via Vesicle-Associated Antibiofilm Activity. MBio, 10(6). doi: 10.1128/mbio.02548-19
[30] Tamir, H., & Srinivasan, P. R. (1970). Studies of the Mechanism of Anthranilate Synthase Reaction. Proceedings of the National Academy of Sciences, 66(2), 547–551. doi: 10.1073/pnas.66.2.547
[31] Li, X. H., Kim, S. K., & Lee, J. H. (2017). Anti-biofilm effects of anthranilate on a broad range of bacteria. Scientific Reports, 17(7). doi: 10.1038/s41598-017-06540-1
[32] Costaglioli, P., Barthe, C., Claverol, S., Brözel, V. S., Perrot, M., Crouzet, M., … Vilain, S. (2012). Evidence for the involvement of the anthranilate degradation pathway inPseudomonas aeruginosabiofilm formation. MicrobiologyOpen, 1(3), 326–339. doi: 10.1002/mbo3.33
[33] Yadav, M. K., Chae, S.-W., Go, Y. Y., Im, G. J., & Song, J.-J. (2017). In vitro Multi-Species Biofilms of Methicillin-Resistant Staphylococcus aureus and Pseudomonas aeruginosa and Their

Host Interaction during In vivo Colonization of an Otitis Media Rat Model. Frontiers in Cellular and Infection Microbiology, 7. doi: 10.3389/fcimb.2017.00125

[34] Guilbaud, M., Bruzaud, J., Bouffartigues, E., Orange, N., Guillot, A., Aubert-Frambourg, A., … Bellon-Fontaine, M.-N. (2017). Proteomic Response of Pseudomonas aeruginosa PAO1 Adhering to Solid Surfaces. Frontiers in Microbiology, 8. doi: 10.3389/fmicb.2017.01465